Fatigue design of expansion joint in ship superstructure

Ruslan V. Guchinsky Sergei V. Petinov
ruslan239@mail.ru spetinov@mail.ru

Abstract

Despite the long history of application of subdivided superstructures and deckhouses, and efforts of ship designers and researchers a sensible solution in design of reliable details at the cut endings was not found yet. It may be explained as consequence of controversial requirements in design of the cut endings.

Fatigue design of the superstructure details is addressed to solution of the problem. Presented is an example of fatigue design of the cut ending in a fast ship superstructure based on application of modified "Strain-Life" criterion for fatigue and subsequent approach which utilizes Neuber's formula and material cyclic properties. To realize the approach a procedure of the long-term stress distribution transformation to the block-type format is developed.

Efficiency of the developed technique is illustrated by comparing the results with those of application standard S-N criteria based techniques. The results of analysis allowed selection of the expansion joint detail of the superstructure geometry and construction procedure providing necessary reliability.

1 General

Subdivision of long superstructures and deckhouses into independent blocks is applied in ship technology for more than a century. The aim of subdivision is to decrease the hull bending stress flow through the superstructures and deckhouses to the longitudinal strength members of ships and to reduce by this the weight of the topside. However, transverse cuts which have to be ended at the main deck of the hull are considered severe stress concentrations with the feasible consequences of early fatigue crack initiation and growth menacing integrity of the hull.

There was a suggestion based on certain evidences that the "Titanic" catastrophe in 1912 was partly due to fracture initiated at the cut in her deckhouse [1]. Recently, fatigue damages were found in the expansion joints of a passenger and naval ships [2, 3].

Although the subdivision of superstructures and deckhouses has a long history of application, the efforts of ship designers and researchers did not result in a sensible solution in design of reliable details at the cut endings at the main deck [4, 5, 6]. It may be explained by a series of controversial requirements in design of the cut ending, such as considering the high stress concentration at the ending, necessity of providing watertightness of superstructure, the problems of layout of structural details and subdivisions inside superstructure block.

2 Fatigue design of the superstructure at the expansion joint

As an example, the problem of reliability of the expansion joint cut ending in the superstructure which emerged in design of the long superstructure of a fast ship was a motivation

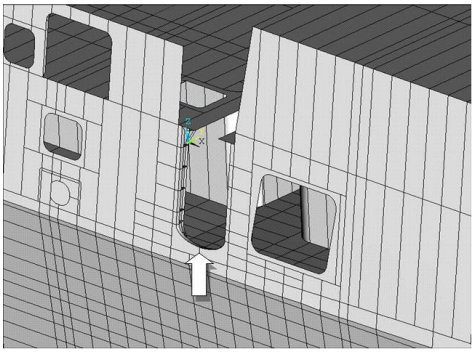

Figure 1: Geometrical model of the ship hull and super-structure at the expansion joint. Arrow shows the critical location

of the present analysis. Characteristic of the ship structure the longitudinal sides of the superstructure are designed as extensions of the ship hull sides. The detail to be considered is the superstructure detail at the base of the expansion joint cutout, shown in Fig.1.

The rules for structural design do not recommend expansion joints in superstructures the vertical longitudinal walls of which coincide with the hull sides, first, by the reason that transverse cuts cause severe stress concentration menacing integrity of the hull structure.

Therefore it was necessary to carry out the due fatigue analysis of the structure, aimed at support the design and providing selection of proper geometry of the bottom part of the cut in the side wall of superstructure. Several versions of the cut ending shape and structural details were considered in the analysis; some of them are indicated in Table 20.

Table 20: Versions of semi-elliptic shape of the cut ending (L* is the length of the semi-elliptic cut ending; H is the minor semi-axis of the cut ending shape

Version	L*, mm	H, mm	L/H	Thickness of the inserted plate at the cut ending, mm	Flange, mm
2	1300	550	2.363	16	80×18
3	1300	425	3.059	16	80×18
4	1400	425	3.333	16	80×18
5	1300	425	3.059	16	80×30
6	1400	425	3.333	16	80×30

Before discussing the procedure of fatigue assessment of the above detail of the superstructure a brief comment to the current principles of fatigue analysis might be appropriate.

3 The principles of fatigue analysis and design of hull structures

Current rules for fatigue strength assessment of ship and marine structures, e.g., [7], etc. require implementation of the linear damage summation, Palmgren-Miner, rule. It covers the widely used approaches, when the S-N criteria, or “Strain-Life” criteria for fatigue

crack initiation are applied, and also when the residual fatigue life is assessed in the crack propagation phase.

The damage summation is recommended to carry out in the common form where the environment loading history is presented as a step-wise histogram:

$$D = \sum_i n_i/N_i = C^{-1} \sum_i n_i \cdot (S_i)^m = N^*/C \sum_i p_i \cdot (S_i)^m \leq \eta \tag{1}$$

where i is the number of equivalent (in the sense of irregular loading is substituted by composition of cyclic loading successions) cyclic stress components in the stress block, n_i is the number of equivalent stress cycles in stress block components, $p_i = n_i/N^*$ is the number of stress "cycles" which the structure should to withstand through the service life, N^* is the fraction of the stress cycles in the life-long loading history attributed to equivalent cyclic stress range S_i , N_i is the number of cycles to failure at constant stress range S_i , η is the "usage factor", total time of exposure to environmental loading related to prescribed service life, C and m are parameters of a fatigue failure criterion, appropriate design S-N curve:

$$N(S) = C/S^m \tag{2}$$

The design S-N curve typically is recommended as a "two-slope" criterion. Evaluation of the equivalent stress range S_i needs in a special comment which is given in the below.

The damage summation scheme (1) also can be accepted in the integral form [8], since the loading history in marine technology is typically given as a continuous stress range probability distribution, (probability density):

$$D = \sum_i n_i/N_i = N^* \int_{Smin}^{Smax} (p(S)/N(S))\, dS \leq \eta \tag{3}$$

This relationship can be readily used to estimate the total fatigue damage, which may be accumulated through service life of a ship or marine structure or, alternatively, the number of stress excursions, N^*, over the intended service life, fatigue life. Also, the allowable stress can be obtained via evaluation of the $p(S)$ parameters on condition the parameters N^* and η are assumed in the analysis.

Alternatively, the fatigue analysis may be carried out applying the "Strain-Life" criterion, frequently with mention of feasible low-cycle fatigue damages to hull structures. However, the criterion and respective procedure of analysis presently are well-developed for application to the whole range, low-cycle and high-cycle fatigue as well.

In the present analysis the "Strain-Life" criterion for fatigue and related technique are applied, taking into account several advantages of the procedure. The principal ones are: the more explicit considering the physical and mechanical nature of fatigue; the more explicit considering the stress concentrations effect on fatigue; in contrast to the S-N criteria-based approaches where the lumped $S - N$ curves are applied regardless the properties of a particular steel, the "Strain-Life" approach takes into account the fatigue and cyclic properties of a steel under the scope.

4 Fatigue assessment of the detail. Strain-life approach

The "Strain-Life" approach includes an appropriate Strain-range-Life criterion and it needs in evaluation of the inelastic (elastic-plastic) strain range at a notch under applied nominal

stress. The latter can be done by using the elastic-plastic cyclic finite-element software; however, even with the present facilities it appears a laborious and timely procedure when a continuous range of nominal stress is accounted. Instead, the rules recommend the use of the Neuber's formula-based technique of evaluation of the local cyclic strain range [9], etc.).

The Neuber's formula-based approach allows approximate solutions at a series of nominal stress ranges characterizing the loading history of the detail. It immediately means that fatigue analysis has to be carried out applying the common damage summation (1); to do this, the equivalent nominal stress range values, S_i , should be defined for every of the step-wise histogram components.

In ship and marine structures design procedures the loading history is presented by the continuous service stress probability function; therefore, it is necessary to transform statistical stress distribution function into equivalent by fatigue damage step-wise histogram. The appropriate technique of transformation is discussed in the following paragraph. Firstly, the statistical parameters of the long-term loading history of the structural detail should be calculated.

In the design stage the loading history may be estimated using a simplified approach via calculation of ship hull (girder) bending moments (in vertical and horizontal planes) in seaway given in the rules and characterized by the recommended probability to exceed.

The long-term probability distributions of bending moments and related stresses are approximated by the two-parameter Weibull formula ([7, 10] etc.):

$$Q(S > S_1) = exp(-(S_1/a_s)^k) \tag{4}$$

which is read as the probability to exceed a stress range S_1; a_s, k are the scale and shape of the distribution parameters, respectively.

The bending moment-induced stresses are used to calculate the scale parameter a_s, the shape parameter, k, can be estimated from the rules by appropriate formulae.

First, the nominal stress is calculated caused by hull bending in vertical plane in the upper strength deck of the hull at location of the detail. The three-dimensional shape of the wave systems involves considering of the hull bending in horizontal plane, too, and calculation of the respective nominal stress at the same location.

The necessary bending moments (given in the rules of DNV [7]) are found from the following equations. Bending moment range in the vertical plane, for the mid-part of the hull:

$$\Delta M_v = 0.30 k_v B L^2 C_w (C_b + 0.257),\ kNm, \tag{5}$$

where k_v is the moment distribution factor depending on the ship's speed; in this analysis $k_v = 1$ for the central part of the hull and moderate speed, L, B are ship length and breadth, respectively, $C_w = 10.75 - (3 - 0.01L)^{15}$ is the effective wave height defined by the bending moment at exceedance $Q = 10^{-8}$, C_b is the block coefficient.

The range of bending moment in horizontal plane, for the mid-part of the hull:

$$\Delta M_k = 0.44 L^{2.25} (d + 0.30B) C_b (1 - cos(2\pi x/L)),\ kNm, \tag{6}$$

where d is the draught in considered load condition.

The respective nominal stress ranges are: due to bending in vertical plane -$S_v = \Delta M_v / W_{min}$, where W_{min} is the section modulus of the hull upper deck, and due to bending in horizontal plane: $S_h = 2M_h/W_h$; W_h is the section modulus of the ship side structure. Since these modes of bending at any moment differ by a random phase angle, the total,

equivalent nominal stress in connection of the deck stringer and sheerstrake is obtained as the sum of random correlated variables:

$$S_{eq} = S_v(1 + (S_h/S_v)^2 + 2\rho_{vh}(S_h/S_v))^{1/2}, \tag{7}$$

where $\rho_{vh} = 1$ is the average value of correlation factor of vertical and horizontal girder bending moments [11].

Scale and shape parameters of the Weibull nominal stress distributions (4) for the ship under the scope: $a_s = S_{max}/(lnN^*)^{1/k}, N^* = \eta \cdot 10^8 = 0.47 \cdot 10^8$, where $\eta = 0.47$ is the "usage" factor, the fraction of service life to be spent on a seaway. The shape parameter, according the DNV rules, is $k = 2.21 - 0.54\ lgL = 1.081$, L is the ship length, molded. The bending moments and nominal stress characteristics at the detail location (probability of exceedance is $Q = 10^{-8}$) are given in Table 21.

Table 21: Bending moments and nominal stress characteristics at the detail location

Plane of bending	Bending moment range, kN*m	Section modulus, m^3	Nominal stress range, MPa	Scale parameter of long-term dis-tribution, MPa
Vertical	$4.719 \cdot 10^5$	1.9961	236.4	16.594
Horizontal	$2.098 \cdot 10^5$	2.8750	73.0	5.124
Equivalent stress, Eqn (7)	—	4.25	254.6	17.872

The stress analysis, specifically detailed at the expected critical location, the superstructure detail at the bottom part of the cut has to be carried out by applying the finite element analysis (FEA). To provide it, a global model of ship hull and superstructure "representative" block to be loaded by design bending moments in vertical (4) and horizontal (6) planes was developed.

The representative block included part of the ship hull and superstructure which is extended from the considered location to the fore and aft parts where another cuts in the superstructure are located. This allows to model behavior of the superstructure blocks, their "opposite bending" induced by the hull bending in vertical plane.

The region of the global model where the cut in superstructure and in particular its bottom is located, is modeled by an essentially fine mesh to provide the necessary stress resolution, Fig.2.

Girder bending moments given in Table 21 were applied to the global model of the representative block and maximum stresses in the flange at the bottom part of the superstructure were calculated.

For the mentioned versions of the shape, semi-elliptical, maximum stresses were calculated. The results, maximum stress values in bending in vertical plane, S_v^{max}, and in horizontal plane, S_h^{max}, are presented in Table 22 together with the statistically equivalent maximum stress ranges calculated using equation (7). Fatigue failure criterion (elastic-plastic cyclic strain-range-life curve) may be taken in the form developed by Manson and Muralidharan [12]:

$$\Delta\varepsilon = 0.0266\varepsilon_f^{0.115}(\sigma_u/E)^{-0.52}N^{-0.56} + 1.170(\sigma_u/E)^{0.852}N^{-0.09} \tag{8}$$

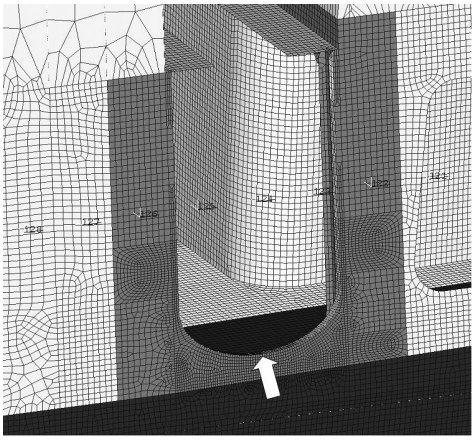

Figure 2: FE modeling of the superstructure in the considered area. Arrow shows the critical location

Table 22: Maximum stress ranges at the cut ending, MPa, and stress concentration factor values for the detail versions considered

Version of the cut shape	2	3	4	5	6
S_v^{max}	539.06	498.95	432.75	472.84	430.60
S_h^{max}	171.20	166.32	150.00	163.90	149.25
S_{eq}^{max}	581.64	538.31	466.94	510.19	464.62
$K_t^{(eq)}$	2.28	2.11	1.85	2.00	1.82

Or, alternatively:

$$\Delta\varepsilon = CN^{-\alpha} + BN^{-\beta} \tag{9}$$

where C, B, α andβ are the best-fit material constants obtained by the cyclic testing of the material samples under the strain range control; N is the number of load cycles.

Parameters of criterion (9) for the steel under the scope (390 Grade higher tensile steel) are: $C = 0.040, B = 0.015, \alpha = 0.653, \beta = 0.140; \sigma_u = 630$ MPa is the tensile strength of the steel [9].

In fatigue analysis of the critical location, the welded joint of the superstructure side plating and the flange, the elastic-plastic cyclic and fatigue strength properties of the base material were applied. Similar properties of the weld material are not available yet. To get at realistic assessment of fatigue resistance of material at critical location the parameter B of the "elastic" term in (9) was modified on condition the due mechanical finishing of the weld material was provided (and the shipyard followed the recommendation). Apart from that, the welded joint resistance was characterized by the appropriate fatigue limit stress amplitude $\sigma_f = 112$ MPa (fully reversed axial cyclic loading; butt weld, ground flush to plate, 100% NDT), as given by Hobbacher [13]). By taking into account effects of irregular service loading as recommended in [14] according which the "offset minimum damaging

stress" should be about , the equation (9) may be rewritten as $\Delta\varepsilon = 1.1\sigma_f/E = CN^{-\alpha} + BN^{-\beta}$ when $N = 10^7$. Taking into account that the fatigue damage develops mostly due to moderate stresses above the mentioned minimum damaging stress the material parameter B characterizing the high-cycle term of the criterion can be estimated:

$$B^* = 1.1\sigma_f N^{\beta}/E - CN^{\beta-\alpha} \tag{10}$$

Apart from that, considering application of the criterion (9) for fatigue assessment of material at a critical location (i.e. at the stress concentration area) it may be rewritten as

$$\Delta\varepsilon = CN^{-\alpha} + B^*N^{-\beta}K_t/K_f \tag{11}$$

where K_f is the fatigue notch factor. The latter may be estimated using Peterson's formula [15]:$K_f = 1 + (K_t - 1)/(1 + g/r)$, in which r is the notch root radius, g is the "structural parameter", approximately equal the size (depth) of the crack initiation area. For the hull steels this parameter is around $g = 0.38(350/\sigma_u)^{1.16}$ (modified Peterson's equation), where $\sigma_u = 630$ MPa, is the tensile strength of the steel.

In the case under the scope effect of the large radiuses in the detail versions diminishes the role of structural parameter in the crack initiation phase. By this reason the fatigue notch factor is approximated by:$K_f \approx 1 + (K_t - 1)/(1.02)$.

The local elastic-plastic strain range values, $\Delta\varepsilon$, are calculated for every of equivalent cyclic loading regimes applying the Neuber's formula, e.g. [9]:

$$\Delta\sigma\Delta\varepsilon = (K_t\Delta\sigma_{eq}^{nom})^2/E = (S_{eq}^{max})^2/E \tag{12}$$

where $\Delta\sigma_{eq}^{nom}$) is the equivalent nominal stress at the every of the equivalent histogram "steps" evaluated as described in above paragraph,E is the modulus of elasticity; the values of theoretical stress concentration factor (equivalent) for every version of the detail are given in Table 22.

To solve equation (12), to define the local strain range, $\Delta\varepsilon$, the experimentally obtained generalized cyclic stress-strain curve for the steel is applied. The necessary fragment of it is presented in Table 23 [9]. The appropriate technique of evaluation the local strain range values using (12) and cyclic curve is described in [9] and elsewhere.

Table 23: Generalized cyclic curve of the 390 Grade steel

$\Delta\varepsilon$	$\Delta\sigma$, MPa	$\Delta\varepsilon$	$\Delta\sigma$, MPa	$\Delta\varepsilon$	$\Delta\sigma$, MPa
0.0005	105.0	0.0030	535.7	0.0055	730.7
0.0010	210.0	0.0035	585.0	0.0060	756.4
0.0015	315.0	0.0040	631.0	0.0065	778.9
0.0020	415.7	0.0045	668.6	0.0070	797.3
0.0025	485.3	0.0050	702.8	0.0075	816.4

Further, the necessary step is evaluation of the step-wise histogram of the stress history for the mentioned structural detail and of the equivalent stress ranges (in the sense of fatigue damage) for every of the histogram steps. The procedure of reducing the long-term stress distribution (4) into a set of cyclic loading successions equivalent by fatigue damaging to the random loading "history" through the service life is described in the below.

5 Description of the procedure

Application of the damage summation rule (1) presumes, as said in above, expressing of the long-term stress range distribution in the form of stress histogram, consisting of blocks of equivalent cyclic loading successions at stress ranges S_i with number of stress repetitions n_i. It is recommended in [7] that the number of equivalent stress successions, "steps", should be selected "large enough to ensure reasonable numerical accuracy, and should not be less than 20...". However, the explicit recommendations on evaluation of representative stress ranges S_i and respective number of stress cycles n_i in every "step" of the block are uncertain.

To solve this problem, a procedure is proposed, as follows. In the context of recommended reducing of the long-term distribution to the block-type composition of equivalent cyclic loading successions, first the partial damages corresponding to every of the steps in the block-type damage summation (1) should be calculated using the general form (3):

$$d_i = N^* \int_{Smin_i}^{Smax_i} (p(S)/N(S))\, dS \tag{13}$$

in which $Smin_i, Smax_i$ are the minimum and maximum stress ranges of the "i" step of the block form (1). Further, the number of equivalent stress cycles in every of the i steps is found as

$$n_i = N^* \int_{Smin_i}^{Smax_i} p(S)\, dS \tag{14}$$

Since the partial damage is defined in the linear summation procedure (1) as $d_i(S_i) = n_i(S_i)/N_i(S_i)$, in which S_i may be regarded an equivalent cyclic stress range of the "i" step, this stress range is obtained conditionally using the partial damage definition and fatigue criterion (2) as:

$$S_{i,eq} = (Cd_i/n_i)^{1/m} \tag{15}$$

Firstly, the maximum equivalent stress distribution parameters should be calculated. The shape parameter of the distribution is defined in above: $k = 1.081$. The scale parameter is obtained through the maximum (once upon the service life) equivalent stress for every of the shape versions, starting from version 2 (shown in Table 21): $a_{eq} = S^{eq}_{max}/(lnN^*)^{1/k} = 581.64/14.246 = 40.829 \approx 40.83$ MPa.

The whole range of stresses for version 2 arbitrary is subdivided into 7 steps: 28-107, 107-186, 186-265, 265-344, 344-423, 423-502 and 502-581 MPa.

For every of steps the relative equivalent number of load cycles (probability of steps in the step-vise ensemble) is calculated using (4) and (14):

$$p_i = n_i/N^* = \int_{S_{min}}^{S_{max}} p(S)\, dS = \frac{k}{a_s^k} \int_{S_{min}}^{S_{max}} S^{k-1} exp(-(S/a_s)^k)\, dS, \tag{16}$$

where S_{min} and S_{max} are stress ranges corresponding to lower and upper boundaries of every of the steps, $N^* = 4.7 \cdot 10^7$ cycles. Results are given in Table 24.

Respectively, for every of the steps the partial damage values are found from (13):

$$d_i = \frac{kN^*}{Ca_s^k} \int_{S_{min}}^{S_{max}} S^{m+k-1} exp(-(S/a_s)^k)\, dS \tag{17}$$

The values of partial damage are also presented in Table 24. Corresponding values of equivalent stress are calculated following (15):

$$d_i = n_i/N_i = n_i S_i^m/C;\ S_i^{eq} = (d_i C/n_i)^{1/m} \tag{18}$$

To carry out calculations, the parameters C, m in (18) were provisionally assumed as for base material [7]: $C = 1.309 \cdot 10^{15}, m = 4$. The results are given in Table 24.

Table 24: Parameters of the step-vise block form of equivalent stress distribution, detail version 2

S class	n_i	p_i	d_i	S_{eq}
28 – 107	$2.140 \cdot 10^7$	0.455	0.231	68.52
107 – 186	$2.492 \cdot 10^6$	0.053	0.680	137.5
186 – 265	$2.480 \cdot 10^5$	$5.270 \cdot 10^{-3}$	0.398	214.1
265 – 344	$2.257 \cdot 10^4$	$4.802 \cdot 10^{-4}$	0. 125	291.8
344 – 423	$1.935 \cdot 10^3$	$4.120 \cdot 10^{-5}$	0.028	371.0
423 – 502	158	$3.370 \cdot 10^{-6}$	0.0049	448.9
502 – 581	12	$2.650 \cdot 10^{-7}$	0.000735	532.1

Further, the equivalent stress values and numbers of cycles for every of the step-wise components of histogram given in Table 24 were used to calculate the total damage index values for every version of the detail geometry. Note that product $K_t \Delta\sigma_{eq,i}^{nom}$ in (12) for every of the histogram steps should be substituted by its equivalent, maximum local stress range, $S_{eq,i}^{max}$.

The same procedure was followed for all of the detail configurations. Respectively, the damage summation was carried out by applying the rule (1). The results are summarized in Table 25.

Table 25: Fatigue damage estimated by the Strain-life method for every version of the detail

Detail version	2	3	4	5	6
Maximum equivalent stress, S_{eq}^{max}, MPa	581.64	538.31	466.94	510.19	464.62
D, damage index	1.128	0.798	0.300	0.530	0.288

It is seen that the versions 4 and 6 of the detail according the analysis reveal the best fatigue resistance, and either of the shape versions can be selected for design and fabrication of the superstructure details. Shipyard followed this recommendation.

It may be important for the purposes of fatigue design philosophy to assess damage for every of the detail geometry by applying the S-N criteria for welded joint of the superstructure side shell and flange bordering shell edge at the bottom of the cut.

6 Fatigue analysis of the detail versions. S-N criteria

The initial step concerns selection of appropriate fatigue criteria for considered detail. The most stressed in the detail is the flange at connection with the superstructure side

shell plating at the bottom part of the cut. Nearly the same stress would develop in the welded joint of the flange and the side shell. Respectively, the two design S-N curves (two-slope curves) are selected in the rules [7], parameters of which are: for welded joint $logC = 12.164, m = 3$ if $N \leq 10^7$ and $logC = 15.606, m = 5$ if $N > 10^7$; for base material $logC = 15.117, m = 4$ if $N \leq 10^7$ and $logC = 17.146, m = 5$ if $N > 10^7$.

In the mentioned rules it is stated that when the joint is parallel to the stress "flow" the stress range calculated for the critical location, in our case the joint of flange and the side shell at the cut bottom, may be reduced by factor 0.9. Further, it is indicated that fatigue resistance of the joint may be increased by machining the weld material [7].

For fatigue analysis the same procedure of reducing the long-term stress probability distribution to the step-wise histogram was applied. The histogram was composed of the same 7 cyclic loading components as in above for every of the detail geometries and the values of $n_i, S_{eq,i}$ given in Table 24 were used to estimate the total fatigue damage by applying the linear damage summation procedure (1):

$$D = \sum_i n_i/N_i = \frac{1}{C}\sum_i n_i S_{i,eq}^m = \frac{N^* S_{o,eq}^m}{C}\sum_i p_i \overline{S}_{i,eq}^m \tag{19}$$

where $\overline{S}_{i,eq}^m = S_{i,eq}^m/S_{0,eq}^m$, and stress range $S_{0,eq}$, was arbitrary selected from Table 24. Respectively, for the base material, shape version 2, on assumption of the one-slope S-N curve (to attain at a rather conservative result), the total damage index is found as $D = \frac{N^* S_{o,eq}^m}{C}\sum p_i \overline{S}_{i,eq}^m = 1.468$

To compare, the total damage was calculated by applying the damage summation in the form of (3) and considering the two-slope form of the S-N curve for the base material. To obtain the stress ranges in the step-vise form of the equivalent stress distribution, the stress range corresponding to the "kink" of the two-slope S-N curve had to be found: $S_0 = (C_1/N_0)^{1/m_1}$. Since the "kink"-stress range was $S_0 = (C_1/N_0)^{1/m_1} \approx 107$ MPa. Consequently, the damage index was found as follows:

$$D = \frac{kN^*}{a_s^k}\left(\frac{1}{C}_1 \int_{S_0}^{S_{max}} S^{m_1+k-1} e^{-(S/a_s)^k}\, dS + \frac{1}{C}_2 \int_{S_{min}}^{S_0} S^{m_2+k-1} e^{-(S/a_s)^k}\, dS\right) = 1.467$$

As it might be expected, the substitution of the continuous equivalent stress distribution by the relative rough, 7 component step-vise histogram results practically in the same value of damage, certainly because of application of the above procedure of reduction the probability stress distribution to the histogram based on equivalence of fatigue damage principle.

However, the results also show that considered version of the cut bottom shape in the superstructure side shell is unacceptable, because the damage index (D = 1.467) predicts the fatigue crack origination within the prescribed service life.

The necessary reliability of the detail as was shown in above Strain-Life-based analysis, may be achieved by decreasing the local equivalent stress. Increasing the cut width (the large axis of semi-elliptic cut bottom shape) by 8% and decreasing the height of its curvilinear part (the minor semi-axis) on around 30% allows decreasing the stress concentration factor value from $K_t^{eq} = 2.28$ to $K_t^{eq} = 1.85$ (the detail version 4).

Similarly, the damage was obtained for every of the detail versions (the bottom of the cut in the superstructure shape); the results are presented in Table 25.

As seen from the Table 26 data, the versions of the detail geometry 4 – 6 may be regarded providing the necessary fatigue life of the considered critical location.

By comparing results of analyses given in Tables 25 and 26 it may be seen that the S-N criterion based technique shows a reasonable qualitative agreement of results with those assessed by Strain-life criterion based approach. Again, the versions 4 and 6 of the detail are characterized by the best fatigue resistance, although the Stress-Life approach application shows somewhat less optimistic estimates of damage for these detail versions. This

Table 26: The reliability characteristics of the detail

Version of the cut shape	2	3	4	5	6
S_v, MPa	539.06	498.95	432.75	472.84	430.6
S_{eq}^{max}, MPa	581.64	538.31	466.94	510.19	464.62
K_t^{eq}	2.28	2.11	1.85	2.00	1.82
The damage, D	1.467	1.062	0.581	0.851	0.568

mismatch may be explained, on the one hand, by implication of elastic material behavior and neglecting effects of microplasticity in the stress concentration areas inherent in the Stress-Life format which overestimates fatigue damage at the critical locations. Apart from this, the format utilizes the "lumped" S-N curves, regardless particular material properties. Respectively, the higher tensile steel fatigue resistance may be underestimated. On the other hand, in application of the Strain-Life methodology it was assumed that material of the detail including welded joint, although machined carefully, was homogeneous, with cyclic stress-strain properties of the parent material, when the "inelastic" term,$CN^{-\alpha}$, of the criterion (11) was considered. As mentioned in above, this might have resulted in moderate underestimation of fatigue damage in the range of infrequent intensive wave loads.

7 Conclusions

1. Fatigue analysis of several versions of the ship superstructure detail at the cut for expansion joint ending allowed selection of sufficiently reliable version of the detail. Analysis was carried out by applying Strain-Life and, as an option, conventional Stress-Life methodologies. Both resulted in a reasonable correspondence of fatigue resistance characteristics of structural details, although the Strain-Life methodology and data base revealed somewhat better fatigue behavior of the detail, mostly due to considering properties of particular steel.

2. To support the analysis a procedure of the continuous long-term stress distribution explicit transformation to the step-vise block-type format is developed. It allows unambiguous evaluation of equivalent cyclic stress fragments and reducing their number compared to those required by the rules for fatigue design and provides accuracy of fatigue analysis of hull and marine structures.

3. Further on, experimental evaluation of cyclic properties and fatigue resistance of welded joint materials would be necessary to improve the data base of the Strain-Life methodology.

Acknowledgements

The authors express their thanks to Mr. A. Ridiger who helped to design the FE-models of the ship hull and superstructure components in the considered area.

References

[1] Deitz, Dan. 1998. How did the Titanic sink? "Mechanical Engineering", ASME

[2] Stapel, H.W., Vredeveldt, A.W., Journee, J.M.J., de Koning, W. 1998. Fatigue Damage in the Expansion Joints of SS Rotterdam. Report 1 166-P, DUT, Delft, Netherlands

[3] Reed, J. (2011) Welding Flaw Led To Crack in LCS-1 Hull. Online Defense and Acquisition Jour-nal. April 11

[4] Chapman, J.C. 1957. The Interaction between a Ship's Hull and a Long Superstructure. Transactions, Royal Institution of Naval Architects. March

[5] Sivers, N.L. 1966. Proektirovanie sudovykh nadstroek [Design of ship superstructures]. Sudostroenie Pubs, Leningrad, SU (In Russian)

[6] Sielski, R.A. 2007. Aluminum Marine Structure Design and Fabrication Guide. USCG Project 1448. Washington, USA

[7] Det Norske Veritas. 2010. Fatigue Assessment of Ship Structures. Classification Notes – 30.7. Hovik, Norway

[8] Bolotin, V.V. 1969. Statistical Methods in Structural Mechanics. Holden-Day, San Francisco, CA.

[9] Petinov S.V. 2003. Fatigue Analysis of Ship Structures. Backbone Publishing Co., Fair Lawn, NJ, USA

[10] Mansour A., Wirsching P., et al. 1997. Assessment of Reliability of Existing Ship Structures. SSC-398, Ship Structure Committee, Washington, USA

[11] Cramer E.H., Loseth R., Oliasen K. and Valsgaard S. 1995. Fatigue Design of Ship Structures. Proceedings, PRADS-95. Seoul, Korea, pp. 2.898-2.909

[12] Manson, S.S, Muralidharan, U. 1988. A Modified Universal Slopes Equation for Estimation of Fatigue Characteristics of Metals. Journal of Eng. Math. and Tech., ASME, Vol.110

[13] Hobbacher A. 2007. Recommendations for Fatigue Design of Welded Joints and Components. IIW Doc. XIII-2151r1-07 / XV-1254r1-07

[14] EUROCODE 3: Design of Steel Structures. Part 1-9: Fatigue. BS EN 1993-1-9: 2005

[15] Peterson, R.E. 1989. Stress Concentration Factors. A Handbook. J.Wiley and Sons, Hoboken, NJ, USA

Ruslan V. Guchinsky, Sergei V. Petinov, Institute for problems in mechanical engineering, Bolshoy pr., 61, V.O., St. Petersburg, 199178, Russia